H. O. Cohn, R. D. McCulloch, W. M. Bugg, G. T. Condo, and M. M. Nussbaum, Phys. Rev. Letters **23**, 146 (1969).

ACKNOWLEDGMENTS

We wish to thank all those whose support, knowledge, and inspiration have helped in the completion of this work.

Thanks are due to the crews of the Bevatron and the 72-in. bubble chamber.

The scanning and measuring efforts, as well as the handling of the many large computer jobs associated with the preliminary data reduction, were supervised by our competent experiment librarians Wally Hendricks, Betty Armstrong, Maureen Nassiri, and Meredeth Vogler. We also owe thanks to the many scanners, and to the supervisors and operators of the Spiral Reader measuring machines.

The staff of the LRL computer center deserve thanks for their constant cooperation throughout the months of data analysis in ensuring fast, reliable processing of hundreds of computer jobs.

We acknowledge the support and encouragement of Professor Luis W. Alvarez.

PHYSICAL REVIEW D VOLUME 2, NUMBER 11 1 DECEMBER 1970

$\pi^- p$ Charge Exchange at Backward Angles*

R. C. CHASE,† E. COLEMAN, H. W. J. COURANT, E. MARQUIT, E. W. PETRASKE,‡ H. F. ROMER,§ AND K. RUDDICK
School of Physics, University of Minnesota, Minneapolis, Minnesota 55455

(Received 17 July 1970)

Results of a measurement of the $\pi^- p$ charge-exchange process at backward angles are presented. Differential cross sections were measured in the angular region $-0.5<\cos\theta^*<-1.0$ at incident momenta of 2, 3, 4, 5, and 6 GeV/c. An additional background subtraction to a version of the data published previously has a significant effect at 6 GeV/c and brings the data into agreement with more recent measurements. The 6-GeV/c data were combined with existing measurements of the differential cross sections for backward $\pi^+ p$ and $\pi^- p$ elastic scattering to yield values for the isotopic-spin-$\frac{1}{2}$ and -$\frac{3}{2}$ u-channel and s-channel amplitudes for backward pion-nucleon scattering and for the magnitude of the phases between them. It is found that the u-channel amplitudes can be explained by pure Regge-pole (Δ_δ,N_α) exchange only near the extreme backward direction, but that a Reggeized absorption model agrees at least qualitatively with the data. The phase difference between the $I=\frac{1}{2}$ and $\frac{3}{2}$ s-channel amplitudes is approximately 90° over the region $-0.8<u<0$ (GeV/c)^2.

I. INTRODUCTION

IN recent years, a number of experiments have shown the existence of pronounced backward peaks in the differential cross sections for the elastic scattering of charged pions from protons.[1] The gross features of the data have been explained rather well by a simple Regge-pole model of nucleon exchange, including only two trajectories.[2]

The $\pi^- p$ backward elastic scattering requires exchange of a doubly charged baryon, and the smooth behavior of the cross section is consistent with exchange of the isotopic-spin $I=\frac{3}{2}$ Δ_δ trajectory. The $\pi^+ p$ backward scattering at incident momenta studied to date, up to 14 GeV/c, is generally larger than the $\pi^- p$ scattering except in the region $u\approx -0.15$ (GeV/c)^2, where u is the square of the four-momentum transfer from incident pion to outgoing nucleon. Near this value of u, the differential cross section for $\pi^+ p$ exhibits a marked dip. The shape of the cross section can be explained by the presence of an additional amplitude from the allowed $I=\frac{1}{2}$ N_α trajectory. Each of these trajectories is well established on a Chew-Frautschi plot. A straight-line extrapolation of the N_α trajectory into the physical scattering region at $\alpha=-\frac{1}{2}$ shows the existence of a wrong-signature nonsense zero in the corresponding amplitude at $u\approx -0.15$ (GeV/c)^2.

* Work supported by the U. S. Atomic Energy Commission under Contract No. AT(11-1)-1764 and by the Graduate School of the University of Minnesota.

† Present address: American Science and Engineering Inc., Cambridge, Mass. 02142.

‡ Present address: Stanford Linear Accelerator Center, Stanford, Calif. 94305.

§ Present address: Department of Physics, University of Washington, Seattle, Wash. 98105.

[1] A. Ashmore, C. J. S. Damerell, W. R. Frisken, R. Rubinstein, J. Orear, D. P. Owen, F. C. Peterson, A. L. Read, D. G. Ryan, and D. H. White, Phys. Rev. Letters **19**, 460 (1967); **21**, 389 (1968); A. S. Carroll, J. Fischer, A. Lundby, R. H. Phillips, C. L. Wang, F. Lobkowicz, A. C. Melissinos, Y. Nagashima, and S. Tewksbury, *ibid.* **20**, 607 (1968); W. F. Baker, P. J. Carlson, V. Chaband, A. Lundby, E. G. Michaelis, J. Banaigs, J. Berger, C. Bonnel, J. Duflo, L. Goldzahl, and F. Plouin, Phys. Letters **23**, 605 (1966); Nucl. Phys. **B9**, 249 (1969); J. P. Chandler, R. R. Crittenden, K. F. Galloway, R. M. Heinz, H. A. Neal, K. A. Potocki, W. F. Pricket, and R. A. Sidwell, Phys. Rev. Letters **23**, 186 (1969).

[2] C. B. Chiu and J. D. Stack, Phys. Rev. Letters **19**, 460 (1967); V. Barger and D. Cline, *ibid.* **16**, 913 (1966); Phys. Rev. **155**, 1792 (1967).

Fits to the charged-pion–proton elastic scattering have been used to determine the strengths of the N_α and Δ_δ trajectory functions and thus enable a prediction to be made for the backward charge-exchange process.[3]

A more critical comparison with the simple Regge theory can be made by combining the measured charge-exchange and $\pi^\pm p$ elastic scattering data to extract values for the magnitudes of the isotopic-spin-$\frac{1}{2}$ and -$\frac{3}{2}$ exchange amplitudes f_{1u} and f_{3u}, respectively, and for the magnitude of the phase difference ϕ between them. Thus, if it is assumed that only u-channel nucleon exchange contributes to backward pion-nucleon scattering, the differential cross sections can be written as

$$\frac{d\sigma}{du}(\pi^- p \to p\pi^-) = f_{3u}{}^2, \tag{1a}$$

$$\frac{d\sigma}{du}(\pi^+ p \to p\pi^+) = (1/9)\,|\,f_{3u}+2f_{1u}e^{i\phi}\,|^2, \tag{1b}$$

$$\frac{d\sigma}{du}(\pi^- p \to n\pi^0) = (2/9)\,|\,f_{3u}-f_{1u}e^{i\phi}\,|^2. \tag{1c}$$

This paper describes an experiment which was designed to measure the backward charge-exchange scattering over a range of incident pion momenta from 2 GeV/c, where s-channel resonant effects appear to be large in the elastic scattering, to 6 GeV/c, where u-channel exchange appears to dominate.

Optical spark chambers were used to detect and measure the recoil angles of the final-state neutron and two γ rays originating from the π^0 decay. Neutrons with momenta close to the incident pion momentum were detected at laboratory scattering angles up to 20°. The corresponding π^0 mesons were scattered in the angular region 120°–180° in the c.m. system, approximately independent of incident pion momentum, and the resulting γ rays were detected at scattering angles greater than 60° in the laboratory system. Measurement of all final-state particle directions enabled overconstrained kinematical fits to be made to each event, thus providing a clearly identified sample of charge-exchange events.

II. EXPERIMENTAL DETAILS

A diagram of the apparatus is shown in Fig. 1.

A. Beam

Negative pions were obtained from the 17° beam of the ZGS (Zero Gradient Synchrotron) at Argonne National Laboratory. Negative kaons and antiprotons were rejected electronically by use of a threshold Čerenkov counter situated at a first focus of the beam.

[3] V. Barger and D. Cline, Phys. Letters **27B**, 312 (1968); Phys. Rev. Letters **19**, 1504 (1967).

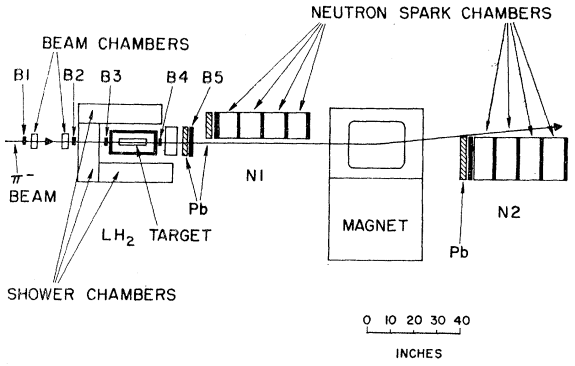

FIG. 1. Experimental layout.

The beam was defined by a scintillation counter telescope, B_1 and B_2, and two thin-foil spark chambers, and focused onto a 12-in.-long liquid-hydrogen target.

B. γ-Ray Detection

The γ rays were detected by the electromagnetic showers produced in brass-plate spark chambers placed on the upstream, left, and right sides of the hydrogen target. These spark chambers had $\frac{1}{8}$-in.-thick plates, with a total thickness of 4 radiation lengths for normal incidence. The plates of the upstream chambers contained 2-in.-diam holes to permit passage of the beam. Inside this assembly was an inner layer of six gaps of low-mass spark chambers. These served to record the passage of charged particles in another phase of the experiment.

Inside the whole array of spark chambers, the target was surrounded by anticoincidence counters in the form of a box of dimensions 8×8×18 in., with the greater dimension in the beam direction. The vertical sides of the box were of 0.5-in. scintillator, while the upper and lower sides consisted of alternate layers of scintillator and lead, with a total thickness of 2 radiation lengths. Lead was also placed at the inner surface of the downstream side of the box. The upstream and downstream faces of the box contained $1\frac{1}{2}$-in.-diam holes to permit passage of the beam. The downstream hole was covered by a 3-in.-diam scintillator $B4$, $\frac{1}{4}$ in. thick.

A further anticoincidence counter $B5$, 10×10 in., was placed in the beam, 12 in. further downstream from the end of the target, preceded by a variable thickness of lead, to detect γ rays from those forward charge-exchange events not detected by the scintillator box.

This array of anticoincidence counters discriminated against neutral final-state events with γ rays emitted at angles less than approximately 60° from the forward direction, or with γ rays passing through the top and bottom of the scintillator box, and thus not through any spark chambers. This latter measure also served to enhance the sample of events with two γ rays, which were less likely to trigger one of the upper or

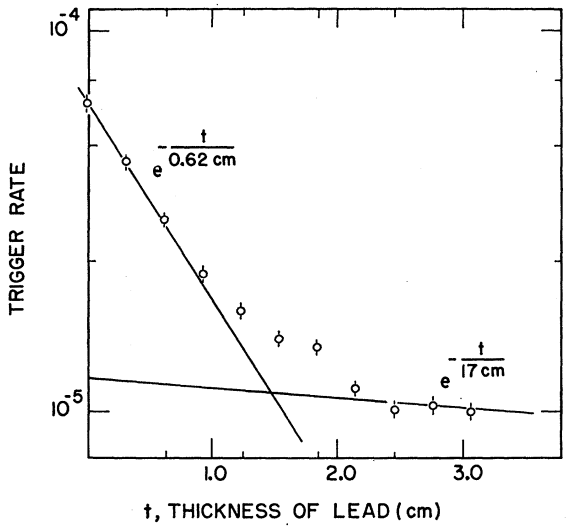

FIG. 2. Distribution of neutron vertices as a function of depth in neutron detector. The fitted exponential yields an absorption length of 17±2 cm and a total interaction probability of 0.92±0.03.

lower veto counters than events with more than two γ rays.

C. Neutron Detection

Neutrons were detected in either of two detectors, $N1$ or $N2$. $N1$ was placed to detect neutrons recoiling at angles between 3° and 20°. $N2$ was placed to detect neutrons scattered at angles less than 6°, including those neutrons scattered directly forward. A C-pole bending magnet was placed between the two detectors to steer beam particles away from $N2$.

The neutron detectors were in the form of four thick-plate spark chambers, each chamber followed by a 1-in.-thick scintillator to detect charged particles from interactions in the spark-chamber plates. Each spark chamber had six gaps and the plates were $\frac{5}{8}$-in. brass. The total thickness of brass in the detector was 17.5 in., corresponding to approximately 2.5 absorption lengths. The thickness of one chamber corresponded to the range of a 200-MeV charged pion.

The light from all four scintillators was piped to a common point via Lucite light pipes, where it was viewed by two photomultiplier tubes. Signals from these tubes were set in coincidence to indicate a possible neutron interaction. The requirement of a coincidence between the signals from the two tubes reduced the possibility of accidental signals.

A separate anticoincidence counter was placed at the upstream end of each neutron detector. This was preceded by a variable thickness of lead which was adjusted empirically at each incident pion momentum to veto triggers from forward-going γ rays not detected by the anticoincidence counters around the target.

D. Optics

A system of front-silvered mirrors was used to obtain two approximately orthogonal views of all the spark chambers. All the chambers were tilted in such a way that the camera viewed the full depth of the gaps.

Fiducial marks consisting of illuminated scratches in Lucite were rigidly attached to the supporting framework, independent of the spark chambers. There were at least five such fiducials in each of the nine independent views. The fiducials were accurately surveyed at the beginning and end of the experiment.

A maximum of one photograph per synchrotron pulse was taken.

E. Data Collection

A photograph was taken whenever the electronics logic circuitry showed that a charged particle had entered the liquid-hydrogen target and a corresponding trigger was obtained from either neutron detector, with no accompanying signal from any anticoincidence counter. A light was flashed to record on film that neutron detector which had been triggered.

Considerable care was taken to ensure that the scintillation counters associated with the neutron detectors detected knock-ons with maximum efficiency. Normally, the four scintillation counters in each neutron detector were viewed together, such that light from all the counters contributed to a signal. The efficiency of a single counter detecting an ionizing particle was checked by blocking off light from the other three counters and examining signals from the passage of beam particles through a single counter in $N2$, and scattered pions in $N1$. Finally, the trigger rate for real events was checked as a function of the high voltage applied to the photomultipliers of the neutron detectors, for a fixed minimum pulse height.

A large background of triggers in the neutron detectors arose from high-energy γ rays from the forward charge-exchange process. This was due to the very small fraction of those γ rays which produced electromagnetic showers penetrating to the first scintillator of the neutron detector, through a thickness of approximately 8 radiation lengths of brass. This background was reduced by placing lead in front of the neutron detector anticoincidence detectors, to convert and thus detect a large fraction of the incident γ-ray flux before it reached the spark chambers. Figure 2 shows a typical plot of the trigger rate as a function of this thickness of lead. The slope of the curve for small thickness of lead corresponds to the conversion length of γ rays in lead, while that slope for greater thickness corresponds to an absorption cross section of approximately 1700 mb for hadrons in lead. Typically, a total of 2.5 cm of lead was used, to convert approximately 99% of the incident γ rays, but only (12±1)% of the neutrons.

At the outset of the experiment, there was found to be a significant fraction of triggers with no visible track in the spark chambers. This background came primarily from a small fraction of those low-energy neutrons from the forward charge-exchange process which interacted in the scintillator of the neutron detector, but which produced knock-ons with insufficient energy to penetrate the first thick plate of the spark chambers. A considerable reduction in this trigger rate was effected by placing typically 2 radiation lengths of lead upstream of the anticoincidence counter $B4$ to convert the associated γ rays which had escaped through the hole of the scintillator just downstream of the target.

The final trigger rate was 2–3 triggers per 10^5 incident pions, depending upon incident momentum. The beam intensity was typically 10^5 pions per synchrotron pulse.

Approximately 20 000 photographs were taken at each of five incident pion momenta, 2, 3, 4, 5, and 6 GeV/c.

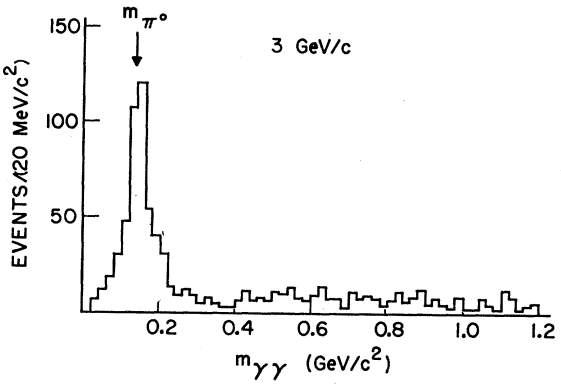

FIG. 3. Effective-mass distribution for γ pairs using one-constraint kinematical fit.

III. DATA REDUCTION AND ANALYSIS

A. Scanning and Measurement

The film was scanned and measured in one viewing on an image-plane digitizer. The size of the image on the table was 20 times the film size, giving a net demagnification of 5. Events were required to have two and only two electromagnetic showers and at least one track from a neutron interaction in the appropriate detector as signaled by the neon indicator lamps. An electromagnetic shower was defined to be a track of at least two sparks, separated by not more than two gaps, and pointing toward the target (within 45° of the target for tracks of three or fewer sparks). A track from a neutron interaction was defined to be any track with two or more sparks, in the proper chamber. About 10% of the film met these requirements and was measured.

A reference coordinate system was established by the measurement of two standard fiducials at opposite sides of the frame. Two points on the beam track, the first spark of the knock-on particle track in the neutron detector, and two points on each γ-shower track were measured for reconstruction. The points measured for the γ showers consisted of the first spark and a second point estimated to be near the center of the shower maximum. A majority of the film was scanned and measured twice.

B. Event Reconstruction

The position in space of the measured points were calculated by a geometrical reconstruction program. The γ-ray-shower tracks were extrapolated to the incoming beam line and the vertex of the event required to lie on that line. The best position of the vertex was computed by weighting the two γ lines by the factor $(l \sin\theta)/d$, l being the distance between the two points measured in the shower, and thus a measure of the momentum, θ being the angle relative to the beam, and d being the distance of the first point on the track from the target. The directions of the two γ's and of the neutron were then defined by vectors from the vertex to the first spark in the shower.

The event was then processed by a kinematic fitting program, based on the standard program GRIND.[4] Measurement of the recoil angles of all the final-state particles leaves three unknowns, the momenta of these particles. The four energy-momentum equations then provide a one-constraint fit to an event if the mass of the two-γ system is left free, and a two-constraint fit if the mass is contrained to be that of the π^0.

The data were first analyzed using a one-constraint fit. A resulting mass spectrum of the two-γ system is shown in Fig. 3. This stage of the analysis demonstrated the existence of π^0 mesons in the data, well separated from a background, arising from a number of sources. In the region close to the π^0 peak, the background is thought to come primarily from misidentified events with final states of $2\pi^0$ or $\pi^0\gamma$ (from ω^0 decay). The events at greater masses come from backward η production, but also from peripheral $K^0\Lambda^0$ and $K^0\Sigma^0$ production with a forward K^0 producing a neutron trigger and the Λ or Σ decaying to an undetected neutron and γ rays.

The uncertainties assigned to the particle recoil angles as input to the fitting program were taken to be the same for all events: $\pm 3°$ for the γ rays, $\pm 0.75°$ for the neutrons in the upstream detector, $\pm 0.25°$ for those in the downstream detector, and $\pm 0.4°$ for the beam. These uncertainties were estimated by consideration of the accuracy of spark location and resulted in reasonably flat χ^2 probability of fit distributions. It was judged that the resolution was sufficiently good that a more detailed procedure of calculating allowed errors for each event was unnecessary.

[4] GRIND Manual, Version VIII, Argonne National Laboratory (unpublished).

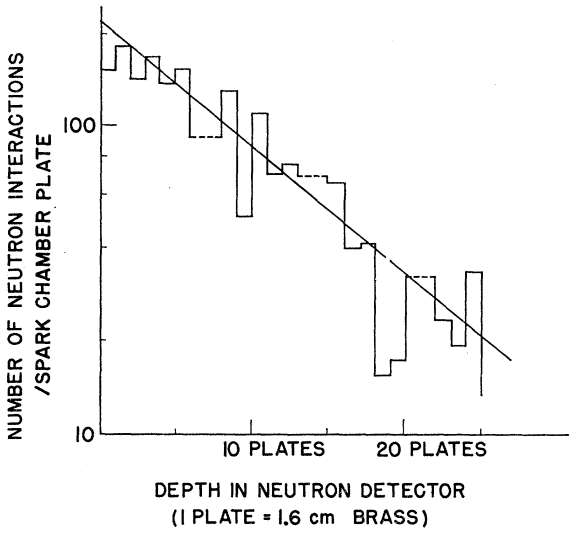

FIG. 4. Event rate in $N2$ as a function of thickness of lead before anticoincidence counter.

It was found that the fitting program gave divergent results for a fraction of apparently genuine charge-exchange events, generally occurring away from the extreme backward direction, where the angles between the γ rays were smaller and the fit much more sensitive to measurement errors. A two-constraint fit to the data, with the assumption that the two γ rays originated from a π^0 meson, yielded an additional 20% of fitted events over the number of acceptable charge-exchange events from the one-constraint fit. About 40% of the measured film was accepted by the fitting program.

From the two scans and measurements of the film, it was determined that the combined measurement and scanning efficiency for two scans was $(82\pm2)\%$, where approximately half the inefficiency was a scanning inefficiency, and half a measurement inefficiency. This efficiency was independent of incident momentum and of neutron scattering angle.

C. Neutron Detection Efficiency

The probability of a neutron interaction in the neutron detectors was determined directly from the distribution of interaction points in the detector. This is shown in Fig. 4, where the data from all incident momenta have been included. The exponential attenuation yields an absorption cross section of 715 ± 50 mb for neutrons in brass, in excellent agreement with other determinations.[5] This cross section yields a total probability of absorption of 0.92 ± 0.03 in the detector. The flattening of the data in Fig. 4 near zero depth in the detector is correlated with a known low spark efficiency for corresponding gaps. Any effect due to backscattering of secondary particles producing signals in the upstream veto counter was less than 5%, and no correction has been made for this effect.

There are several effects which could depress the actual neutron detection efficiency below the interaction probability. These will be discussed in some detail.

(i) Interaction products could be produced at such large angles, near the edge of the detector, that they missed the scintillator. The maximum loss from such an effect must be 50% for production of a single particle, while for production of two particles the loss is 25% for interactions occurring at the extreme edge of the detector. The actual average number of secondary particles was determined by inspection of vertices from fitted events. It varied from 1.16 to approximately 2.0 for neutron momenta between 2 and 6 GeV/c, respectively. The edge effects were checked directly by an inspection of the neutron vertex distribution across the face of the detectors. For a fixed neutron scattering angle, the vertex density was constant within the statistical accuracy for all azimuthal angles of the neutron to within approximately 1 in. of the edge of the detector. The regions of the neutron detector in which neutrons from the charge-exchange reaction could interact was determined primarily by the geometry of the γ-ray detection spark chambers. In general, neutrons interacted at least 2 in. inside the edges of the detectors except in the extremes of the overlapping areas of the two detectors, between 3° and 6° neutron scattering angle, and for the extreme forward-scattered neutrons where the detector $N2$ extended at least 2 in. beyond the direct line of the incident beam. The cross sections deduced from each detector in the overlap region are in excellent agreement and have been combined in the data presented here. The data corresponding to neutrons scattered at less than 1° in the laboratory show no difference within the statistical accuracy between those scattered to the right or left, and these have also been combined.

(ii) The probability that a neutron will suffer an elastic scattering in the detector is of the same order as the absorption probability. Thus, a neutron may be scattered from the detector before an absorption process occurs. The first diffraction minimum for a 2-GeV/c neutron elastically scattered from a copper nucleus occurs at approximately 4° scattering angle and thus might be expected to have an appreciable effect only for neutrons passing within approximately 1 in. from the edge of the detector at 2 GeV/c, and closer to the edge at higher momenta. As already described no data with a neutron interaction closer than 1 in. to the edge of the detector were used in the analysis.

(iii) Reaction products may have insufficient energy to reach the scintillator in the detector, since material between adjacent scintillators in the detectors amounted to the range of a charged pion with momentum approxi-

[5] T. Coor, D. A. Hill, W. F. Hornyak, L. W. Smith, and G. Snow, Phys. Rev. 98, 1369 (1955); J. H. Atkinson, W. N. Hess, V. Perez-Mendez, and R. W. Wallace, Phys. Rev. Letters 2, 168 (1959).

mately 300 MeV/c. A direct check on this source of loss was made by measuring the number of spark-chamber plates penetrated by each secondary particle produced in those events with a neutron identified by kinematic fitting.

We found that at 2-GeV/c incident pion momentum the median number of plates penetrated by a single knock-on particle was 6, and that the average number of secondary particles per interaction was 1.16. The average range of the secondaries appears to increase approximately in proportion with the momentum of the interacting neutron from 2 to 4 GeV/c, while the average number of knock-ons increases to 1.4 at 4 GeV/c. This multiplicity is consistent with the average numbers of pions produced in nucleon-nucleon interactions observed in bubble chambers.[6] The energy distribution is consistent with the notion that the secondary particles are mainly pions coming primarily from an isotropic distribution of pions produced in the c.m. system of the incident nucleon with a single nucleon in the copper nucleus, with an average c.m. pion momentum of approximately 200 MeV/c.

TABLE I. The results of Monte Carlo calculations for the probability for detection of the two γ rays from π^0 decay and of the neutron in detectors $N1$ and $N2$ from the backward charge-exchange reaction. The results are shown as a function of θ_n, the neutron laboratory scattering angle, and of u, the square of the four-momentum transfer from incident pion to outgoing neutron. The results are shown only for the lowest and highest momenta of the experiment and have been normalized to the same neutron detection efficiency of 0.92 to demonstrate the variation of the γ-ray detection. The results at 2 GeV/c must be multiplied by a factor 0.77 to obtain the absolute detection efficiency.

Incident momentum	θ_n (deg)	u ((GeV/c)^2)	$P(N1)$	$P(N2)$
2 GeV/c	1.5–3.0	0.151		0.350
	4.5	0.136	0.260	0.195
	6.0	0.113	0.258	0.119
	7.5	0.083	0.250	
	9.0	0.046	0.240	
	10.5	0.002	0.225	
	12.0	−0.047	0.208	
	13.5	−0.098	0.190	
	15.0	−0.164	0.166	
	16.5	−0.230	0.137	
	18.0	−0.300	0.104	
	19.5	−0.374	0.070	
	21.0	−0.451	0.037	
6 GeV/c	1.0–2.0	0.033		0.360
	3.0	−0.017		0.270
	4.0	−0.091	0.226	0.220
	5.0	−0.188	0.233	0.192
	6.0	−0.308	0.238	0.118
	7.0	−0.449	0.243	
	8.0	−0.608	0.248	
	9.0	−0.786	0.253	
	10.0	−0.980	0.257	
	11.0	−1.19	0.260	
	12.0	−1.41	0.265	
	13.0	−1.63	0.260	
	14.0	−1.88	0.246	
	15.0	−2.12	0.226	

[6] G. F. Chew and A. Pignotti, Phys. Rev. 176, 2112 (1968).

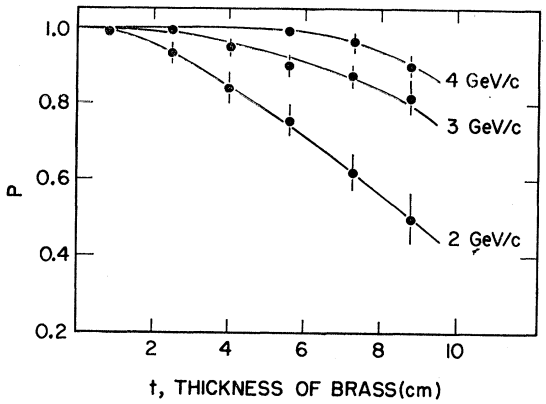

FIG. 5. Probability P for detection of at least one reaction product from a neutron interaction after a thickness of brass t following the interaction.

Figure 5 shows the probability of detection of at least one particle from a neutron interaction as a function of range in the brass-plate spark chambers. These curves were calculated by integration of the knock-on range spectra, taking into account the average number of particles produced.

When the data of Fig. 5 were integrated over the amount of material between adjacent scintillators, it was found that losses amounted to (23±5)% at 2 GeV/c, (10±3)% at 3 GeV/c, and less than 2% at higher momenta.

D. Geometrical Detection Efficiency

A Monte Carlo program was used to determine the probability that the two γ rays from the decay of the π^0 meson would be detected in the experimental arrangement. For fixed neutron scattering angles, this program generated events with a random neutron azimuthal angle and with isotropic decay of the π^0 in its rest frame.

The possible directions of the γ rays were defined by the edges of the lead-scintillator anticoincidence counters above and below the target, and by a hole in the extreme backward direction, to remove fake events arising from spurious sparks produced along the edges of the hole in the upstream spark chambers. The program included the probability of conversion of at least one γ ray in the target or thin-plate spark chambers before reaching the brass-plate spark chambers (typically 10%), and also the probability that at least one γ ray would pass through the brass chambers without conversion (typically 10%). The conversion length in the chambers was calculated from the known radiation length in brass and from the known dependence upon γ-ray energy. The chambers consisted of sufficient conversion lengths that the energy dependence of conversion produced only a small effect on the detection efficiency, approximately 5% for the lowest-momentum π^0 mesons.

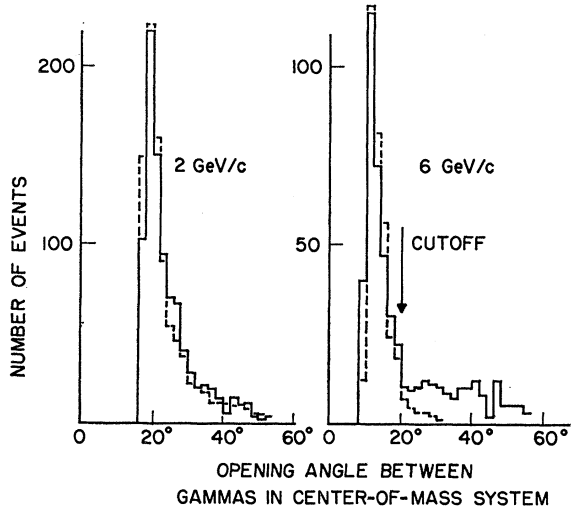

FIG. 6. Distribution of opening angles between γ pairs in c.m. system. The solid lines are the data. The broken lines represent the distributions predicted by Monte Carlo calculation with the experimental resolution folded in.

The probability of detection of the two γ rays and of the neutron in detectors $N1$ and $N2$ is shown in Table I for incident pion momenta of 2 and 6 GeV/c, as a function of neutron scattering angle. This represents the principal correction to the data and demonstrates the angular dependence of this correction.

E. Other Corrections

In addition to the corrections already described, some additional corrections were made.

Curves of counting rate as a function of the pressure in a Čerenkov counter at the first focus of the beam showed that electron contamination in the beam was negligible. Muon contamination was measured by bending the beam into the downstream neutron detector $N2$ and scanning the film for interactions as a function of depth in the detector. The resultant curves were fitted to an exponential attenuation of pions with a constant fraction of muons in the beam. This latter was found to be $(2.5\pm1.0)\%$ at all incident momenta.

Runs were made at 3 and 5 GeV/c with the hydrogen target empty. The background from this source was $(5\pm2)\%$, consistent with the amount of matter in the target windows. This is to be compared with the actual empty-target trigger rate which was 20% of the full-target rate. The difference was due to interactions in the beam counters and to other spurious triggers.

Absorption of incident pions in $B2$, in the air, and target amounted to $(2.2\pm0.2)\%$. The fraction of pions decaying between B2 and the target was 0.3% at 2 GeV/c, less at higher momenta. Dead time due to anticoincidence counters was $(1\pm1)\%$.

F. Final Data Selection

As a check on the event selection, a study was made of the distribution of opening angles of the two γ rays in the c.m. system of the neutron and neutral pion. The data are shown in Fig. 6 for incident pion momenta of 2 and 6 GeV/c. Also included in the figure is that distribution predicted by the Monte Carlo program with the experimental resolution folded in. It can be seen that the data at the higher momentum include an excess of events with large opening angles. These are presumably events from processes other than the charge-exchange process. Any other reactions producing a neutral pion in the backward direction such as $\pi^-p \to K\Lambda^0$ or $\pi^-p \to n\pi^0\pi^0$ give pions of lower momenta than those from the charge-exchange process and thus yield greater opening angles between the two γ rays. A cut was made on the opening angle distribution, accepting only those events having a two-γ opening angle of less than twice the minimum for the 6-GeV/c data, to three times the minimum at 2 GeV/c. Background removed by this cut was only significant at 5 and 6 GeV/c. A Monte Carlo calculation was made to determine the correction required by this cut, typically 5–10% depending on neutron scattering angle.

This background subtraction was not made in an earlier version of the data.[7]

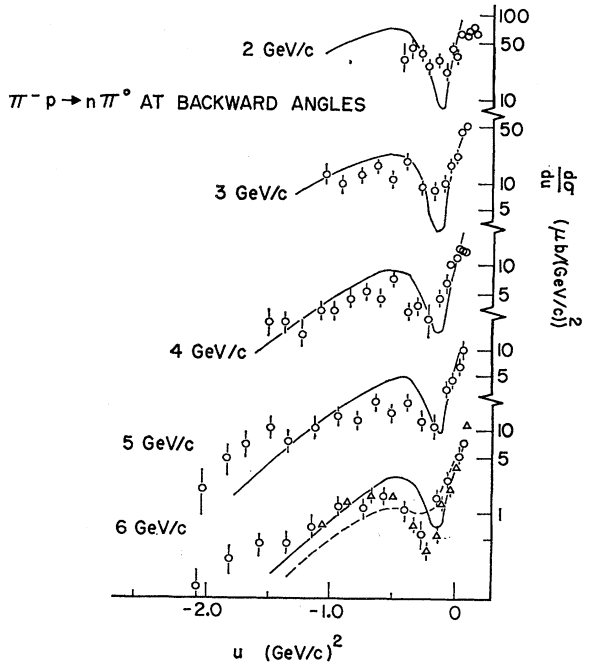

FIG. 7. The experimental data, including those of Boright *et al.* (Ref. 9) at 6 GeV/c. The solid curves are predictions of a Regge-pole-exchange model; the broken curve at 6 GeV/c is a calculation using a Reggeized absorption model of the process.

[7] R. C. Chase, E. Coleman, H. W. J. Courant, E. Marquit, E. W. Petraske, H. F. Romer, and K. Ruddick, Phys. Rev. Letters 22, 1137 (1969).

TABLE II. The experimental data.

	$\cos\theta_n$	u ((GeV/c)^2)	$\frac{d\sigma}{d\Omega}$ (μb sr^{-1})	$\frac{d\sigma}{du}$ (μb (GeV/c)$^{-2}$)	% error
2.0 GeV/c	0.994	0.151	15.5	64.6	15
	0.984	0.136	18.1	75.5	10
	0.969	0.113	16.7	69.6	10
	0.949	0.083	14.7	61.4	11
	0.925	0.046	14.7	61.4	10
	0.896	0.002	8.20	34.2	13
	0.863	−0.047	10.4	43.4	11
	0.826	−0.098	5.60	23.4	15
	0.786	−0.164	7.89	32.9	13
	0.742	−0.230	6.67	27.8	15
	0.696	−0.300	9.16	38.2	16
	0.647	−0.374	10.6	44.2	24
	0.596	−0.451	8.42	35.1	33
3.0 GeV/c	0.992	0.096	20.0	51.8	12
	0.980	0.064	17.7	45.8	9
	0.961	0.018	8.66	22.4	13
	0.935	−0.043	6.53	16.9	15
	0.905	−0.117	3.87	10.0	18
	0.869	−0.194	3.40	8.8	18
	0.828	−0.313	3.51	9.1	17
	0.783	−0.412	6.95	18.0	12
	0.734	−0.531	4.75	12.3	15
	0.682	−0.658	6.56	17.0	13
	0.627	−0.791	5.08	13.2	17
	0.569	−0.928	4.07	10.6	22
	0.510	−1.07	5.46	14.2	25
4.0 GeV/c	0.996	0.075	8.46	15.8	17
	0.989	0.052	9.10	17.0	15
	0.979	0.017	7.14	13.3	12
	0.965	−0.030	6.26	11.7	12
	0.948	−0.087	3.41	6.36	19
	0.927	−0.155	2.38	4.45	21
	0.904	−0.232	1.43	2.68	41
	0.878	−0.319	1.89	3.54	21
	0.850	−0.415	1.73	3.23	21
	0.819	−0.519	3.90	7.29	14
	0.785	−0.630	2.48	4.64	17
	0.750	−0.748	2.74	5.12	16
	0.713	−0.872	2.59	4.84	16
	0.675	−1.00	1.71	3.20	20
	0.635	−1.13	1.64	3.06	22
	0.594	−1.27	0.80	1.50	33
	0.552	−1.41	1.17	2.19	30
	0.509	−1.56	1.15	2.15	33
5.0 GeV/c	0.995	0.052	7.43	10.9	15
	0.987	0.017	4.43	6.52	17
	0.975	−0.036	3.20	4.70	14
	0.958	−0.106	2.47	3.63	16
	0.938	−0.192	0.82	1.20	30
	0.915	−0.293	1.08	1.59	24
	0.888	−0.408	1.78	2.62	18
	0.858	−0.537	1.35	1.98	19
	0.825	−0.678	1.74	2.56	16
	0.789	−0.830	1.14	1.68	19
	0.751	−0.992	1.23	1.81	18
	0.711	−1.16	0.94	1.38	20
	0.670	−1.34	0.56	0.83	27
	0.627	−1.53	1.01	1.48	20
	0.582	−1.71	0.51	0.74	30
	0.537	−1.91	0.36	0.54	38
6.0 GeV/c	0.995	0.033	5.83	7.00	16
	0.985	−0.017	4.35	5.23	17
	0.971	−0.091	2.32	2.79	15
	0.952	−0.188	1.55	1.80	18
	0.929	−0.308	0.50	0.59	34
	0.902	−0.449	0.90	1.08	26
	0.871	−0.608	1.47	1.77	19
	0.837	−0.786	1.14	1.36	21
	0.800	−0.980	1.16	1.41	19
	0.760	−1.19	0.60	0.72	26
	0.718	−1.41	0.41	0.49	30
	0.674	−1.63	0.40	0.48	30
	0.628	−1.88	0.26	0.31	34
	0.581	−2.12	0.12	0.14	58

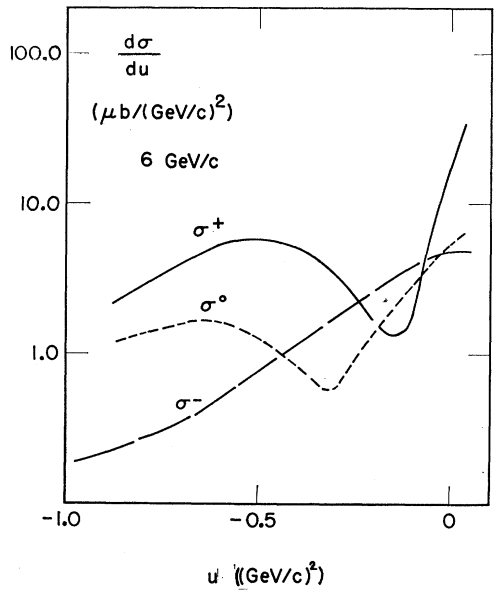

FIG. 8. A comparison of the backward charge-exchange differential cross section σ^0 with the cross sections for backward π^+p and π^-p elastic scattering, σ^+ and σ^-, respectively, at 6 GeV/c incident pion momentum. The elastic scattering data are those of Ashmore *et al.* (Ref. 1).

IV. RESULTS AND DISCUSSION

A. Results

The data are plotted in Fig. 7 and are presented in tabular form in Table II. The curves shown superimposed on the data are theoretical calculations of the process. The solid lines represent a prediction of the cross section by Barger and Cline[3] using a simple Regge model including exchange of N_α and Δ_δ trajectories with residues determined from their fits to the elastic scattering data; the dashed curve at 6 GeV/c represents a fit by Kelly, Kane, and Henyey[8] to our preliminary data[7] using a Reggeized absorption model. Also shown in the figure are the recent data of Boright *et al.*[9] at 6 GeV/c. In addition, the data are in good agreement with data of Schneider *et al.*[10] which cover only a limited u region near the backward direction. At 4 GeV/c, the data at large u agree well with preliminary results from a measurement covering the intermediate angular region between the large forward peak in the cross section and the present measurements in the backward region.[11] A measurement of the 180° differential cross section as a function of incident pion momenta gives results in the low-momentum region (2–4 GeV/c) which are systematically higher than the data presented here.[12]

The most significant feature of the data is the existence of a dip near $u \approx -0.3$ (GeV/c)^2. The dip appears more pronounced in the present data than in our preliminary data[7] due to the presence of a small background which appeared in the latter data for incident momenta of 5 and 6 GeV/c, as described in Sec. III F.

At an incident momentum of 6 GeV/c, the maximum attained in this experiment, any contribution from direct-channel amplitudes should be minimal, and elastic scattering data by Ashmore *et al.*[1] exist with comparable statistical accuracy. The main features of the elastic scattering and charge-exchange reactions are illustrated in Fig. 8.

Values for the magnitudes of the isotopic-spin-$\frac{1}{2}$ and -$\frac{3}{2}$ u-channel exchange amplitudes f_{1u} and f_{3u}, respectively, and for the magnitude of the phase ϕ between them, have been determined using Eqs. (1) and are plotted in Fig. 9. The errors shown in the data of Fig. 9 correspond to statistical errors and also include the effect of a possible 20% normalization error between the charge-exchange data and the elastic-scattering data. This analysis cannot at present be made at other momenta above 3 GeV/c, where u-channel exchange

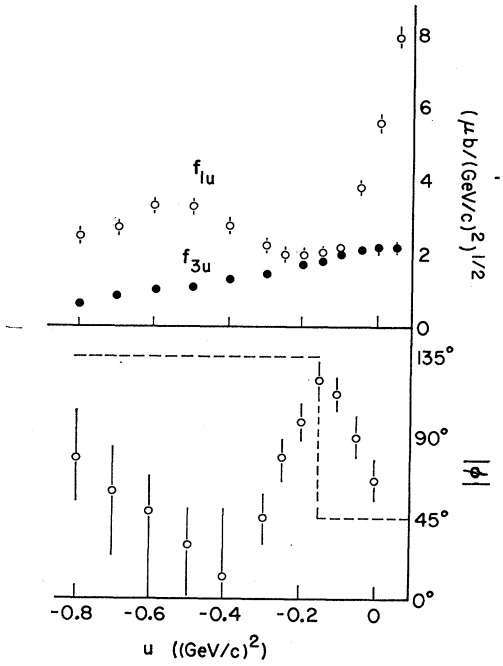

FIG. 9. The isotopic-spin-$\frac{1}{2}$ and -$\frac{3}{2}$ u-channel exchange amplitudes and the magnitude of the phase between them, for backward pion-nucleon scattering at 6 GeV/c. The broken line represents the prediction of the pure Δ_δ, N_α Regge-pole-exchange model.

[8] R. L. Kelly, G. L. Kane, and F. Henyey, Phys. Rev. Letters **24**, 1511 (1970).

[9] J. P. Boright, D. R. Bowen, D. E. Groom, J. Orear, D. P. Owen, A. J. Pawlicki, and D. H. White, Phys. Rev. Letters **24**, 964 (1970).

[10] J. Schneider, V. Lepeltier, P. Bonamy, P. Borgeaud, O. Guisan, and P. Sonderegger, Phys. Rev. Letters **23**, 1068 (1969).

[11] C. R. Sullivan, W. S. Brockett, G. T. Corlew, W. R. Frisken, T. L. Jenkins, A. R. Kirby, J. A. Todoroff, and W. B. Richards, Bull. Am. Phys. Soc. **15**, 42 (1970).

[12] V. Kistiakowsky, R. K. Yamamoto, R. D. Klem, P. Mareato, A. Romano, D. G. Crabb, A. C. Meyers, III, and J. R. O'Fallon, Phys. Rev. Letters **22**, 618 (1968).

may dominate, because of a lack of elastic $\pi^- p$ scattering data.

B. Regge-Pole Exchange

The baryon-exchange Regge-pole model of Barger and Cline[3] includes contributions from both N_α and Δ_δ trajectories, corresponding to exchange of isotopic spin $\frac{1}{2}$ and $\frac{3}{2}$, respectively, and has been very successful in describing the sharp dip in the elastic $\pi^+ p$ scattering. The N_α pole amplitude has a zero at $u=-0.15$ GeV/c^2, resulting in a dip in the differential cross section near that value of u, while the amplitude for the Δ_δ exchange does not have a zero near the extreme backward direction, thus explaining the lack of structure in the pure $I=\frac{3}{2}$ exchange process of backward $\pi^- p$ scattering. From Fig. 9(a) it is seen that the magnitude of f_{1u} falls rapidly, away from the backward direction, going through a minimum at $u\approx -0.15$ (GeV/c)^2 where, however, the magnitude of f_{1u} is similar to that of f_{3u}.

A more sensitive test of any model is provided by a comparison between the predicted phase between the f_{1u} and f_{3u} amplitudes and the magnitude of that phase determined here. In terms of the Reggeized exchange model, the phase of an amplitude is determined by the factor $(1+\tau^{-i\pi(\alpha-1/2)})$, where $\tau=\pm 1$ is the trajectory signature, and by the sign of the residue function which determines the over-all sign of the amplitude. If exchange of only Δ_δ and N_α trajectories contributes to the process at small u, the phase difference ϕ between those amplitudes should be $+45°$ for an angular momentum spacing $\alpha_\Delta-\alpha_N=0.5$ between the trajectories. When the N_α amplitude goes through zero at $u=-0.15$ (GeV/c)^2, its phase advances by 180°, giving a phase difference $\phi=-135°$ for $|u|\gtrsim 0.15$ (GeV/c)^2.

The behavior of ϕ predicted by the N_α, Δ_δ exchange model is seen in Fig. 9(b). It can be seen that there is agreement with the data only near the extreme backward direction.

The model could be made to yield the correct phase difference ϕ up to $u\approx -0.2$ (GeV/c)^2 by the addition of another established isotopic-spin-$\frac{1}{2}$ trajectory N_γ, which lies an additional one-half unit of angular momentum, approximately, below N_α and which does not have a zero near the backward direction. At $u=-0.15$ (GeV/c)^2, the phase difference ϕ should then be 90°.

The existence of a contribution from N_γ exchange can be checked by inspection of the s dependence of the differential cross sections for the backward elastic and charge-exchange scattering at $u=-0.15$ (GeV/c)^2. A compilation of the existing data[1] is shown in Fig. 10. The differential cross sections for $\pi^- p$ and $\pi^+ p$ elastic scattering and the $\pi^- p$ charge-exchange scattering should be in the ratio of 1:1/9:2/9 for pure $I=\frac{3}{2}$ exchange, determined from the Clebsch-Gordan coefficients appearing in Eqs. (1). Since the Δ_δ is the highest lying of the baryon trajectories, it should dominate at high s with the cross sections showing an s dependence of s^{-2}. Although the statistical accuracy of the data is limited, the behavior of the cross sections at $u=-0.15$ (GeV/c)^2 is qualitatively as expected, with considerable structure at low s, from the effect of direct-channel resonances. For a component due to to N_γ in the $\pi^+ p$ elastic scattering and charge-exchange reactions, the differential cross sections should be in the ratio of 4:1, respectively, and the s dependence should be $s^{\alpha 2(u)-2}\approx s^{-4}$ in the low-s region, where the N_γ contribution dominates. The s dependence of the $\pi^+ p$ scattering is $\approx s^{-7}$ for incident momenta between 2 and 6 GeV/c. Thus, inclusion of a contribution from the N_γ trajectory cannot give the correct s dependence of the differential cross sections at $u=-0.15$ (GeV/c)^2.

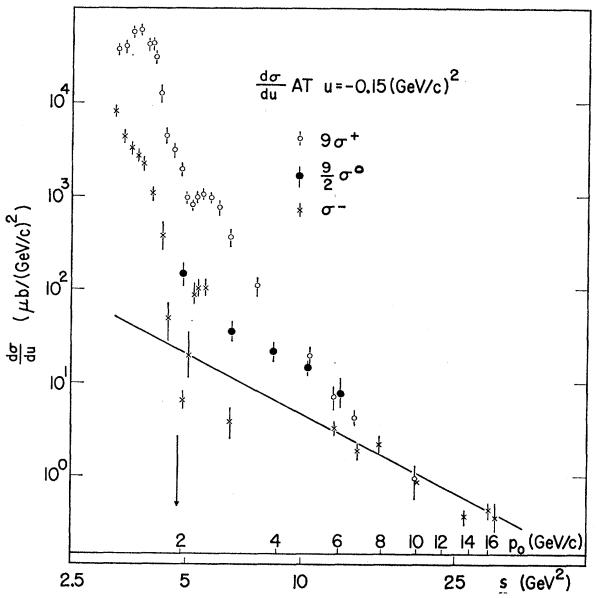

FIG. 10. The differential cross sections σ^+, σ^-, and σ^0 at $u=-0.15$ (GeV/c)^2 as a function of s, the square of the total c.m. energy. For pure isotopic-spin-$\frac{3}{2}$ exchange, the values of $9\sigma^+$, σ^-, $\frac{9}{2}\sigma^0$ should be the same.

C. Reggeized Absorption Model

The model of Kelly, Kane, and Henyey[8] gives a very different explanation of the dips seen in the processes involving isotopic-spin-$\frac{1}{2}$ exchange amplitudes. The pole amplitudes do not have wrong-signature nonsense zeroes. The dips occur near that value of u where the magnitude of a strong cut amplitude, approximately 180° out of phase with the corresponding pole amplitude, becomes equal to the pole amplitude. Thus, the phase difference ϕ between the f_{1u} and f_{3u} amplitudes should be 45° near the backward direction and again approximately 45° when the cut terms from both the Δ_δ and N_α trajectories dominate. Thus, this model appears to give at least qualitative agreement with the data.

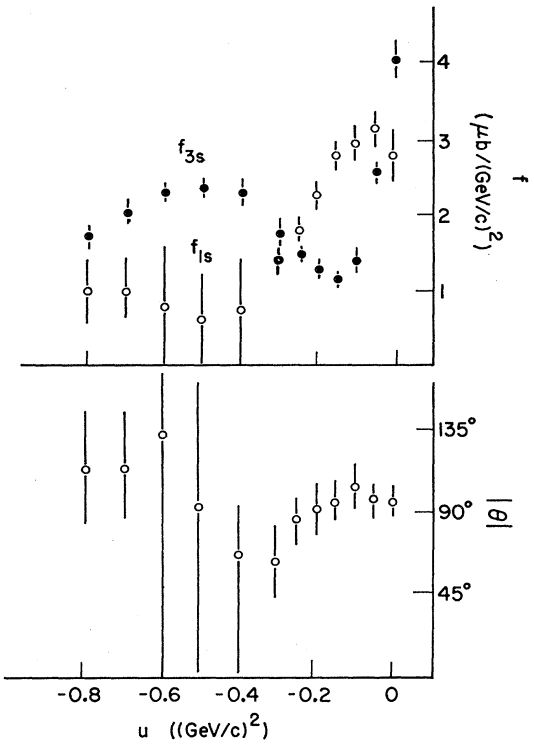

FIG. 11. The isotopic-spin-$\frac{1}{2}$ and -$\frac{3}{2}$ direct-channel amplitudes, and the magnitude of the phase between them, for backward pion-nucleon scattering at 6 GeV/c.

D. Further Discussion

In order to study the s-channel behavior of the backward pion-nucleon processes, we have obtained values for f_{1s} and f_{3s}, the isotopic-spin-$\frac{1}{2}$ and -$\frac{3}{2}$ s-channel scattering amplitudes, respectively, and for the magnitude of the phase difference θ between them, by using the relations

$$\frac{d\sigma}{du}(\pi^- p \to p\pi^-) = (1/9)(f_{3s}+2f_{1s}e^{i\theta})^2,$$

$$\frac{d\sigma}{du}(\pi^+ p \to p\pi^+) = f_{3s}{}^2,$$

$$\frac{d\sigma}{du}(\pi^- p \to n\pi^0) = (2/9)(f_{3s}-f_{1s}e^{i\theta})^2.$$

The data are shown in Fig. 11. The s-channel amplitudes are related to the u-channel amplitudes f_{1u} and f_{3u} through crossing symmetry. Thus

$$f_{1s} = -\tfrac{1}{3}f_{1u}+\tfrac{4}{3}f_{3u},$$
$$f_{3s} = \tfrac{2}{3}f_{1u}+\tfrac{1}{3}f_{3u}.$$

A striking feature of these data is the constancy of the phase difference θ between f_{1s} and f_{3s}. Apart from a region where the magnitude of θ is essentially indeterminate with the present accuracy of the experiments, the phase difference is 90° between the two amplitudes. It cannot be ascertained whether the sign of this phase changes near $u=-0.5$ (GeV/c)^2, corresponding to a similar uncertainty in the phase between the u-channel amplitudes, but it appears reasonable to assume that the phase remains constant over the entire region $-0.8<u<0$ (GeV/c)^2. If it is assumed that the phases of the u-channel amplitudes are correctly predicted by Regge theory at the extreme backward direction, with $\phi_{3u}-\phi_{1u}\approx+45°$, then f_{1s} must lead f_{3s} by 90° on an Argand diagram, i.e., $f_{1s}\approx if_{3s}$.

With 90° phase difference between f_{1s} and f_{3s}, the differential cross sections for the various backward pion-nucleon processes are given by the sums of the squares of the amplitudes f_{1s} and f_{3s}, with the appropriate Clebsch-Gordan coefficients. It can be seen that the dip in the backward π^+p scattering cross section corresponds to the dip in f_{3s} at $u=-0.15$ (GeV/c)^2 but that the dip in the charge-exchange reaction occurs at the crossover point between the f_{1s} and f_{3s} amplitudes near $u=-0.3$ (GeV/c)^2. The lack of structure in the π^-p scattering cross section corresponds to the fact that the terms $f_{1s}{}^2$ and $4f_{3s}{}^2$ change at approximately the same rate in opposite senses.

There appears to be no simple explanation of the forms of the s-channel isotopic-spin amplitudes. Crittenden *et al.*[13] have been able to reproduce the form of the f_{3s} amplitude, and thus the shape of the backward π^+p differential cross section for incident pion momenta between 2 and 5 GeV/c, by summing the amplitudes from a series of $I=\frac{3}{2}$ resonances using truncated Breit-Wigner forms for the resonance amplitudes. Since the $I=\frac{3}{2}$ resonances have positive parity, this leads to a predominantly real, negative amplitude for f_{3s} at the higher momenta, above that region where individual resonances dominate the amplitude. The $I=\frac{1}{2}$ direct-channel amplitude is more complicated since cancellation occurs between contributions from even- and odd-parity resonances. The resultant amplitude at high incident momentum must still be predominantly real, either positive or negative. It might be argued that cancellation between the real parts of the amplitudes could lead to a predominantly imaginary amplitude, thus explaining the magnitude of the phase difference between f_{1s} and f_{3s} found here. This is unlikely, however, since such cancellation should lead to a small f_{1s} amplitude while the f_{1s} and f_{3s} amplitudes are found to be similar in magnitude. Thus, it appears that such a model is unable to produce the required magnitudes of the amplitudes in addition to the required phase difference.

The data presented here provide no information on the helicity amplitudes involved in the backward pion-nucleon processes. Preliminary measurements have

[13] R. R. Crittenden, R. M. Heinz, D. B. Lichtenberg, and E. Predazzi, Phys. Rev. D 1, 169 (1970).

been made of the polarization parameter P for backward $\pi^+ p$ elastic scattering at incident momenta below 3.75 GeV/c.[14] The polarization shows significant variation over the momentum interval studied.

Since, at 6-GeV/c incident momentum, the relative phase between the f_{1s} and f_{3s} amplitudes remains constant over the region $-0.8<u<0$ (GeV/c)^2, it follows that any difference in phase between the nonflip and flip components of the amplitudes must be the same for both the f_{1s} and f_{3s} amplitudes. It also follows that any change in the phase of the f_{1s} amplitude produced by a change in the relative magnitudes of the two helicity components of f_{1s} must be exactly followed by a corresponding change in the phase of the f_{3s} amplitude. Thus, the polarization in all backward pion-nucleon processes at 6-GeV/c incident momentum must be similar in both magnitude and sign.

[14] R. Miller and A. Yokosawa, Argonne National Laboratory Report No. ANL/HEP 7001, 1970 (unpublished).

ACKNOWLEDGMENTS

We wish to extend our thanks to the entire ZGS staff for their kind cooperation and assistance toward the successful completion of the experiment, and also to our able staff of scanners under the leadership of Jerry Wright. We have had the advantage of a great many discussions with our theoretical colleagues at the University of Minnesota.

PHYSICAL REVIEW D VOLUME 2, NUMBER 11 1 DECEMBER 1970

Kaon-Nucleon Total Cross Sections from 0.36 to 0.72 GeV/c*

T. Bowen, P. K. Caldwell,† F. Ned Dikmen, E. W. Jenkins, R. M. Kalbach, D. V. Petersen, and A. E. Pifer

Department of Physics, University of Arizona, Tucson, Arizona 85721

(Received 16 July 1970)

The K^+ and K^- total cross sections were measured on both hydrogen and deuterium at a series of momenta between 360 MeV/c and 720 MeV/c by the transmission method. The data were corrected for Coulomb and decay effects, and the isospin states were extracted. The K^+N, $I=1$ cross section was found to be free from resonances, although the presence of a small dip at about 700 MeV/c was confirmed. No convincing evidence was found for structure in the K^+N, $I=0$ cross section, which was observed to be steeply rising with increasing momentum throughout this range. The prominence of the $\Lambda'(1520)$ was verified in the K^-N, $I=0$ system in which no additional structure was seen. In the K^-N, $I=1$ system no new structure was clearly established, though there appears to be a small enhancement with a mass about 1600 MeV.

I. INTRODUCTION

In recent years, very accurate measurements have been made on the $K^\pm$-nucleon total cross sections above a laboratory momentum of 1000 MeV/c.[1–4] The experiment by Bugg *et al.*[4] measured these cross sections above 600 MeV/c with typical errors of ± 0.2 mb. However, below 700 MeV/c their errors vary between ± 0.4 and ± 1.9 mb. Below 600 MeV/c,[5,6] previous measurements have errors of 2–3 mb, except for a recent K^-p bubble-chamber experiment[7] with errors of ± 1 mb, and no accurate judgment of the detailed behavior of the total cross section could be made.

It was decided to measure the total cross sections of charged kaons on hydrogen and deuterium to a statistical accuracy of about 1% in the region 350–720 MeV/c. This precision was judged necessary in order to reevaluate the S-wave scattering and effective-range parameters at very low energies. In addition it was thought possible that one or more yet undetected kaon-nucleon resonant structures might exist in the mass range 1500–1660 MeV. Only the $\Lambda'(1520)$ had previously been seen in the K^-p total cross section[6] and no structure at all had been detected in the K^+p total cross section.

* Work supported in part by a grant from the National Science Foundation.

† Present address: Physics Department, University of Michigan, Ann Arbor, Mich. 48104.

[1] R. L. Cool, G. Giacomelli, T. F. Kycia, B. A. Leontić, K. K. Li, A. Lundby, and J. Teiger, Phys. Rev. Letters **16**, 1228 (1966).

[2] R. L. Cool, G. Giacomelli, T. F. Kycia, B. A. Leontić, K. K. Li, A. Lundby, and J. Teiger, Phys. Rev. Letters **17**, 102 (1966).

[3] R. J. Abrams, R. L. Cool, G. Giacomelli, T. F. Kycia, B. A. Leontić, K. K. Li, and D. N. Michael, Phys. Rev. Letters **19**, 678 (1967).

[4] D. V. Bugg, R. S. Gilmore, K. M. Knight, D. C. Salter, G. H. Stafford, E. J. N. Wilson, J. D. Davies, J. D. Dowell, P. M. Hattersley, R. J. Homer, A. W. O'Dell, A. A. Carter, R. J. Tapper, and K. F. Riley, Phys. Rev. **168**, 1466 (1968).

[5] S. Goldhaber, W. Chinowsky, G. Goldhaber, W. Lee, T. A. O'Halloran, and T. F. Stubbs, Phys. Rev. Letters **9**, 135 (1962).

[6] M. B. Watson, M. Ferro-Luzzi, and R. D. Tripp, Phys. Rev. **131**, 2248 (1963).

[7] R. Armenteros, P. Baillon, C. Bricman, M. Ferro-Luzzi, E. Pagiola, J. O. Petersen, D. E. Plane, N. Schmitz, E. Burkhardt, N. Filthuth, E. Kluge, H. Oberlack. R. R. Ross, R. Barloutaud, P. Granet, J. Meyer, J. P. Porte, and J. Prevost, CERN Report No. D. Ph. II/PHYS. 70-7 (unpublished).